SEISMIC MODELING OF A REINFORCED SLOPE

Gordon Fung, EIT, Ender Parra & John P. Sully, P. Eng.
MEG Consulting Ltd, Richmond, British Columbia, Canada
John R. Kerr, P. Eng., Regional Manager
Tensar International Corporation, Calgary, Alberta, Canada
Kenneth P. Akins, P.E., Manager of Technical Services
Tensar International Corporation, Alpharetta, Georgia, United States

ABSTRACT
This paper presents the seismic modeling performed for the design of a 9-m high 70° reinforced slope with an upper 2H:1V fill slope of up to 4 m high. The Sierra Slope, a reinforced soil slope using geogrids, was introduced by Tensar International Corporation (Tensar) in 1982. The FLAC (Fast Lagrangian Analysis of Continua) finite difference program was used to model the Sierra Slope under seismic loading conditions. FLAC analyses are considered to provide an evaluation of the standard design approaches and an insight into the seismic performance of the Sierra Slope.
RESUMEN
El articulo presenta el modelaje sismico de un muro armado de 9 m de altura con talud de 4 m encima. El muro es un product Sierra Slope de Tensar. Se ha realizado el analisis numerico de diferencias finitas con el program FLAC para evaluar el metodo AASHTO tipico tradicional de diseno para este tipo de muro.

1 INTRODUCTION

The 9-m high reinforced slope will be constructed in the Lower Mainland, British Columbia, Canada. The Sierra Slope was designed by Tensar and MEG Consulting Ltd. (M+EG). As with the traditional design approach for the proprietary Sierra Slope design, Tensar analyzed the combined (external and internal) stability of the slope and M+EG analyzed the global stability and performed the numerical modeling.

Based on the design requirements for soil-structure interaction analysis, a dynamic finite difference program has been used to model the seismic response of the reinforced slope. The reinforced slope was designed to provide acceptable seismic performance during a seismic event with 5 percent probability of being exceeded in 50 years, which corresponds to a return period of 975 years. The slope design is in accordance with the AASHTO standard guidelines. Specific performance requirements for the reinforced slope under the design earthquake loading require that:

- collapse prevention with limited access to emergency traffic;
- significant damage and permanent deformations are permitted, but no collapse or losses of primary supports are allowed.

The paper considers the case of a wall built on a potentially liquefiable layer. To satisfy the specific performance requirements, the Sierra Slope was designed to be found on ground improvement (stone column) zone. In addition, the length and the spacing of reinforcements are determined to achieve the limit equilibrium factor of safety requirements.

2 GEOTECHNICAL ASPECTS

A geotechnical investigation was conducted for the site. The geotechnical study aimed at evaluating the soil properties for the foundation and design of the subject structure and other adjacent structures proposed for the project as well as assessing the site specific seismic response of the soils.

2.1 Stratigraphy

According to the Geological Survey of Canada Map No. 1484A, the native soils found at the site are part of the Fraser River Sediments (F_c, F_d) geological unit underlain by Capilano Sediments (C_e) and Pre-Vashon Deposits (P_{vf}, P_{vg}). The representative soil stratigraphy at the site as interpreted by M+EG consists of an upper layer of sandy fill overlying a 3 m thick layer of silt underlain by a 15 m thick layer of loose to compact silty sand to sand, followed by 15 m of dense sand, which in turn overlies deposits of clayey silt and till-like soils.

2.2 Ground Water

Seasonal variation of groundwater table was estimated from piezometer monitoring in the range of El. +0.5 m to El. +2.2m above sea level. An average groundwater elevation of El. +1.5 m was used in the geotechnical analyses. The Sierra Slope is to be founded at elevations ranging between El. +3.4 m and El. +5.4 m above sea level.

2.3 Ground Improvement

In order to mitigate the liquefaction potential of the loose to compact silty sand to sand layers when subjected to earthquake events with return periods of 475-yr, 975-yr and subduction, stone columns formed by vibro-replacement methods were installed under the base of the Sierra Slope to a depth of 20 m below the existing ground.

To minimize post-construction settlements due to consolidation of the upper 3m thick silt layer and lower clayey silt at 35 m of depth under applied loads, a 1.5 m high temporary preload surcharge will be placed on top of the Sierra Slope immediately after its completion.

3 NUMERICAL MODELING

The finite difference software FLAC Version 6.0 (Itasca 2008) was used to perform the 2D nonlinear dynamic analyses of the reinforced slope. This was the current version of FLAC during the period of time this analysis was performed. FLAC simulates nonlinear behavior by a generalized finite difference model, allows large-strain formulations, has built-in constitutive models, allows the use of interface and structural elements and uses a stable explicit solution method that marches-on in time. The FLAC analyses are based on effective stresses with no coupled flow (no drainage) in the analyses. Details of the soil and structural input properties used in the FLAC analyses are described in the following sections.

The purpose of the numerical modeling was to assess the performance of the reinforced slope under seismic loading conditions. Results of the FLAC analyses include horizontal and vertical displacements of the reinforced slope and forces in the geogrids during and after a design earthquake. The results provide an insight into the performance of the Sierra Slope under earthquake loading.

3.1 Soil Properties

The soil properties used for the analyses are based on the results of a geotechnical investigation including in-situ and laboratory tests. The shear wave velocity measurements were also used to obtain a better assessment of the moduli of the soils. A summary of the geotechnical parameters used in the FLAC analyses are presented in Table 1. Each layer in the soil profile was considered to be homogeneous. The soil layers used in the model are illustrated on Figure 1.

Since the existing foundation soils are considered to be susceptible to liquefaction during seismic events, the saturated granular soils are modeled using the UBCSAND liquefaction constitutive model (Byrne 2007) that incorporates the liquefaction behavior of granular materials.

3.2 Calibration of Soil Models

For cohesive and unsaturated granular materials, a Mohr-Coulomb elastic-plastic model with FLAC built-in hysteretic damping model (sig3) was used. The parameters for the sig3 model were selected to match the

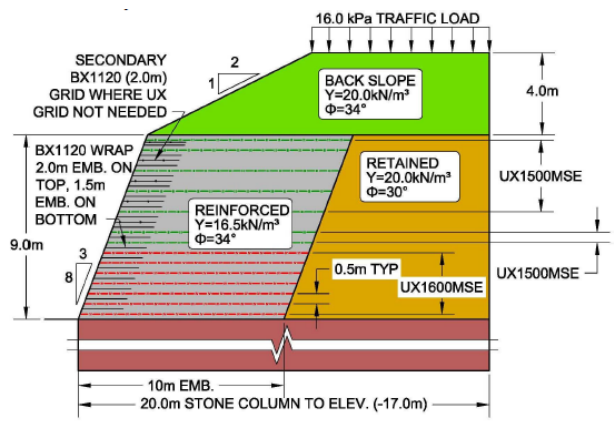

Figure 1. Soil profile and Sierra Slope geometry used in FLAC analyses.

G/G_{max} and damping (versus shear strain) curves presented by Vucetic and Dobry (1991) for cohesive soils and EPRI (1993) for sands. A comparison of the G/G_{max} and damping (versus shear strain) curves obtained from the FLAC sig3 model and those from the referenced literature are presented on Figure 2. The agreement between the two curves is generally very good up to shear strains of about 1%. Table 1 presents the input parameters for the FLAC sig3 model.

The saturated granular materials were modeled using the dynamic liquefaction model UBCSAND. The UBCSAND model was calibrated using the field data obtained from the standard penetration test (SPT) and the cone penetration test (CPT) based on nearby site explorations. It should be noted that all the recommended correction factors have been applied to determine the final $[(N_1)_{60cs}]$ values, except that the correction for not using sample liners and non-standard borehole diameters have not been applied. On the other hand, an upper bound $K\sigma$ correction has been used and the overall effect on $[(N_1)_{60cs}]$ values should be relatively small.

The equivalent clean sand corrected SPT blow count $[(N_1)_{60cs}]$ was found to vary with depth in the sand layer from 15 to 25 at the specific study site. For the granular soils, the dilation angle was estimated to be about $[(N_1)_{60cs}]/10$, as recommended for use with the UBCSAND model. The equivalent SPT blow count and the dilation parameters are defined as those needed to match the curve derived from liquefaction case histories, as suggested by Seed et al. (1985).

Table 1. Soil properties used in the FLAC analyses

Soil Description	Total Unit Weight (kN/m^3)	Shear Modulus (MPa)	Poisson Ratio, υ	Friction Angle, ϕ (^{o})	Undrained Shear Strength, Su (kPa)	FLAC Sig3 Model *			UBCSAND model
						a	b	xo	$(N_1)_{60cs}$
Granular FILL	18.5	19 - 48	0.30	32	-	1.011	-0.6	-1.485	-
SM/ML	16.7	44 - 68	0.40	-	50	1.017	-0.65	-1.411	-
SG	19.0	76 - 80	0.30	35	-	-	-	-	30
Medium dense SP	18.6	80 - 128	0.30	33	-	-	-	-	15 - 17
Dense SP	19.0	131 - 174	0.30	35	-	-	-	-	25
CL-ML	18.0	165	0.45	-	85	1.042	-0.7	-1.231	-
CL	18.0	134	0.45	-	85	1.078	-0.773	-0.614	-
CL-GC	20.0	149	0.45	-	140	1.017	-0.65	-1.411	-

* a, b and x0 are constants used in the FLAC Sig3 Model.

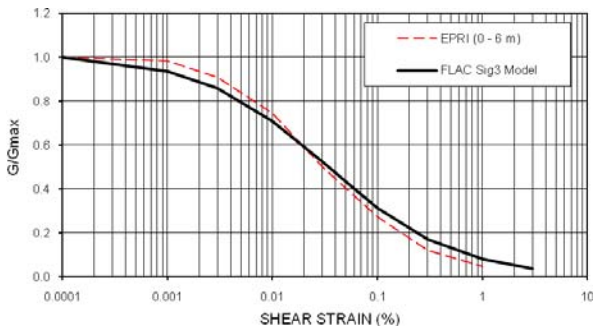

(a)

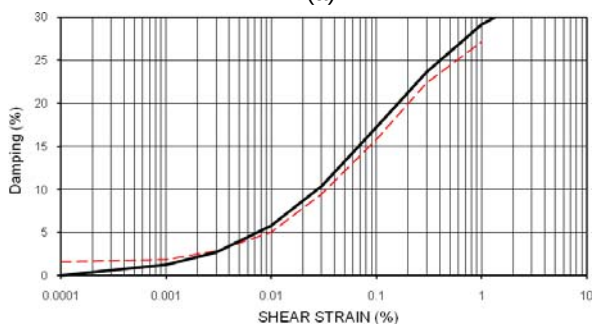

(b)

Figure 2. Published curves versus FLAC sig3 model (a) G/G_{max} curves and (b) Damping curves.

A comparison of the prediction of the occurrence of initial liquefaction based on the UBCSAND model and the case histories presented by Seed et al. (1985) is presented on Figure 3.

For the stone-column reinforced sand layer, a minimum $[(N_1)_{60cs}]$ value of 30 was used for a normalized magnitude of 7.5. The improvement factor defined to achieve this increase in N value was also used to increase the shear modulus of the soil. A summary of the constitutive models for each of the soil layers that are used in the FLAC analyses is presented on Table 1.

3.3 Calibration of 1D Site Response Analyses

For the FLAC analyses, the input acceleration records were de-convoluted using SHAKE to a depth corresponding to the base of the FLAC model placed at a depth equal to the assigned basal layer. The soil models described above were used in FLAC to perform an equivalent 1D site response analysis that was compared with the results from both SHAKE and DESRA. The till-like material has been taken to be representative of a Class C site, with an average shear wave velocity of 600 m/s.

SHAKE and DESRA are equivalent linear and nonlinear codes, respectively, that are widely used for 1D site-specific seismic response analyses. It should be noted that the UBCSAND pore pressure model was not used in the FLAC 1D model since liquefaction was not considered in the 1D site response analysis comparisons.

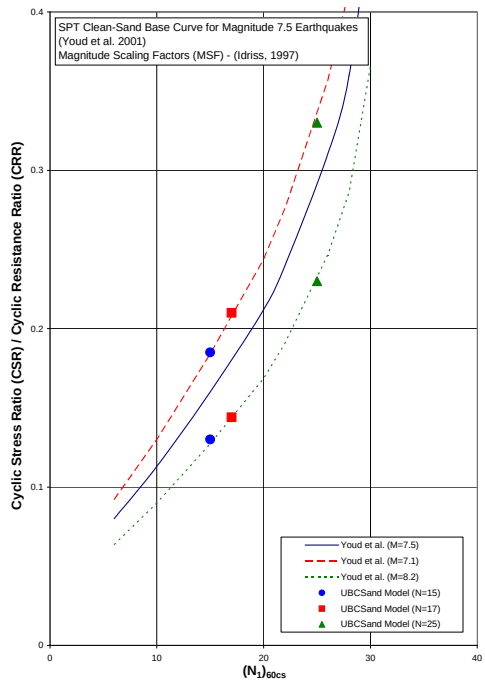

Figure 3. Calibration of UBCSAND model against liquefaction case histories.

The material (Rayleigh) damping at small strain for the FLAC analyses was also calibrated to obtain the best-possible match between the response spectra obtained using FLAC, SHAKE and DESRA. The Rayleigh damping for the FLAC model was estimated to be about 2.5%. The results from SHAKE, DESRA and FLAC including the response spectra and time histories are summarized and presented on Figure 4.

3.4 Structural Properties

The reinforcement (geogrid) is modeled as a strip element and programmed in FLAC Version 6.0. The structural properties used in the FLAC analyses are summarized in Table 2.

The Sierra Slope in the FLAC analyses consists of 3 types of geogrids. The primary reinforcements are composed of Tensar Uniaxial Geogrids (UX1500MSE & UX1600MSE) extending from the slope facing 10 m into the soil mass (i.e. a ratio of length to effective wall height of about 0.71). Tensar Biaxial Geogrids (BX1120) have been used as secondary reinforcement and also act as the Sierra Slope facing, wrapped behind the wire mesh facing.

3.5 Model Construction

The FLAC model was built in stages to provide a realistic representation of the construction conditions. The existing ground conditions and ground improvement zone were modeled to define the initial conditions. Following the establishment of the initial conditions, the reinforced slope was built incrementally in lifts for each layer of geogrid installation. Finally, a time history of earthquake

motion was applied to simulate the seismic loading condition. The FLAC model was constructed as large as practically possible to minimize the edge effects from the boundary of the model.

Table 2. Structural properties used in the FLAC analyses

Properties	Symbol	Units	FLAC Input		
			UX1500MSE	UX1600MSE	BX1120
Width	w	mm	1330	1330	4000
Thickness	t	mm	0.544	0.710	0.225
Density	ρ	kg/m^3	950	950	900
Elastic Modulus	E	GPa	2.28	2.364	1.46
Tensile yield strength	fy	kN	102.6	129.6	17.1
Tensile ultimate strength	fu	kN	114	144	19
Vertical Spacing	Sv	m	0.5/1.0	0.5	0.5
Initial apparent friction coefficient at the interface	f_0	-	0.8	0.8	0.8/1.0 *
Minimum apparent friction coefficient at the interface	f_1	-	0.55	0.55	0.8
Transition confining pressure (if any)	σ'_{co}	kPa	60	70	40
Tensile failure strain limit	-	%	11	11	15

* Initial apparent friction coefficient was taken as 0.8 between BX1120/BX1120 interface and 1.0 between BX1120 and soil.

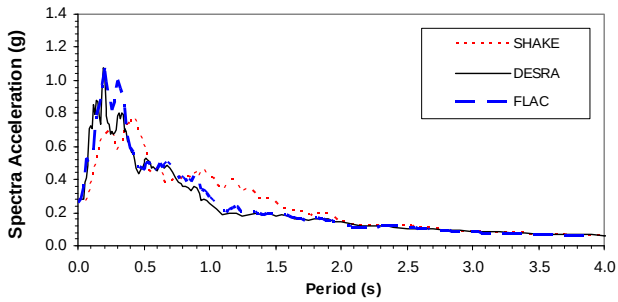

(a)

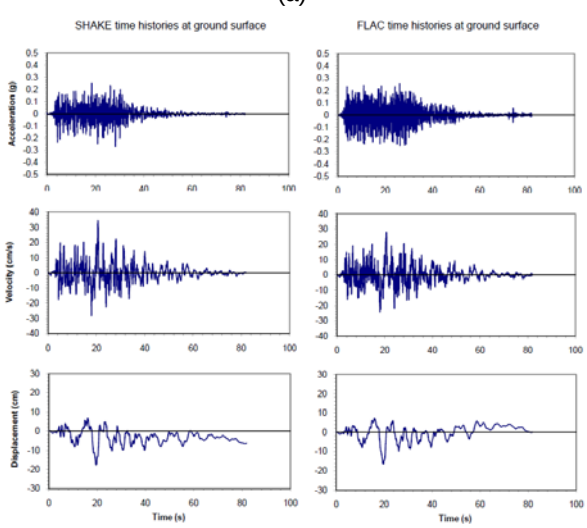

(b)

Fig. 4. Comparison of 1D site response analyses. (a) Surface response Spectra and (b) surface time histories.

The static boundary conditions are modeled as fixed in the horizontal direction for both left and right sides of the model; the base is fixed in both the horizontal and vertical conditions. Free-field boundary conditions were assigned to the sides of the model during seismic analyses while the base was fixed in the vertical direction with the time history velocity record applied in the horizontal direction.

4 RESULTS OF FLAC ANALYSES

Three spectrally-matched earthquake records with two horizontal components have been used as an input in the FLAC analyses. The average of the six earthquake time-history records has been used to evaluate the liquefaction assessment, residual displacements and the tensile forces in the geogrids under the 975-year design earthquake. A performance check was also completed using the 475-year records to ensure that the performance requirements were satisfied.

4.1 Liquefaction Assessment

The liquefaction assessment was evaluated using the FLAC analyses and was compared to the traditional approach where triggering of initial liquefaction is estimated based on the recommendations published by Youd et al. (2001). Liquefaction assessments are typically performed using an equivalent-linear 1D dynamic analysis program such as SHAKE. The results of the SHAKE analyses provide the variation with depth of the cyclic stress ratio (CSR) which is compared to the cyclic resistance ratio (CRR) of the soil based on penetration test data (CPT or SPT).

The FLAC analyses indicate that the extent of liquefaction is less than that determined by the SHAKE analysis approach. For the 975-year earthquake analyses, the FLAC analysis indicates that initial liquefaction occurs from El. -3.5 m to El. -8 m; however, the SHAKE analysis approach predicts that the liquefaction zone will extend to El. -15 m. This is particularly the case for the subduction earthquake where the simplified methodology appears to exaggerate the impact of the subduction event. It would appear that the parameters used to adjust the simplified method for the subduction event with greater numbers of cycles and longer duration are overly conservative, compared to the FLAC results.

The FLAC analyses also provide the time when initial liquefaction occurs. The timing of the initial liquefaction is important when evaluating the lateral displacements of the Sierra Slope. Code-based approaches may significantly overestimate the expected deformation since the combined post-seismic approach (liquefaction and/or post-seismic degradation plus inertial forces) assumes that liquefaction occurs before the onset of the strong motion. The lateral deformations will be significantly increased when the liquefaction has occurred at the beginning of the strong motion, compared to at some time after the strong motion part of the record has passed. Under these conditions the ground deformations from FLAC are generally lower than those obtained from the combined seismic analyses based on a softened soil and the Newmark approach. The difference is particularly pronounced for lower levels of shaking.

For the 975-year earthquake analyses with FLAC, the results indicate that liquefaction occurs shortly after the

passage of the strong motion component as shown on Figure 5.

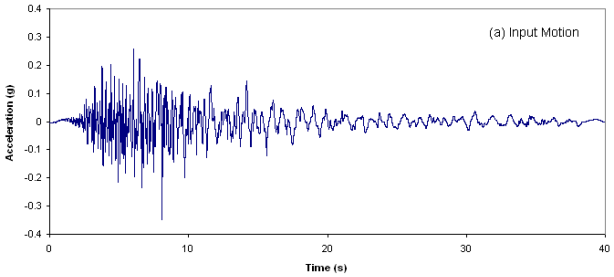

(a)

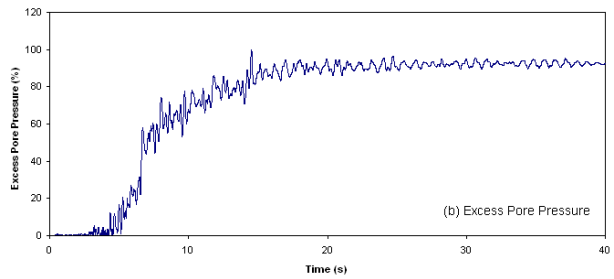

(b)

Figure 5. (a) Input ground motion for Loma Prieta earthquake and (b) Excess pore pressure generated from UBC Sand model in FLAC analysis.

4.2 External Stability

The calculated lateral deformations from the FLAC analyses have been compared to the simplified approach detailed in the Applied Technology Council publication ATC-49. The simplified approach of estimating lateral deformations includes the use of limit equilibrium slope stability and Newmark (1965) deformation analyses.

Newmark considered that the lateral deformations are generated by the unbalanced sliding forces when the factor of safety of a slope is temporarily less than 1.0 under seismic conditions. The limit equilibrium slope stability analyses were used to estimate the yield acceleration (the minimum acceleration required to produce instability of the slope) of the mobilized surface during the seismic event. The acceleration record was then integrated to obtain the permanent deformations.

The failure surfaces from both the limit equilibrium stability and FLAC finite difference analyses are presented on Figure 6. The average deformations from the FLAC analyses are 420 mm (lateral) and 175 mm (vertical) at the top of the front face of the reinforced Sierra Slope. The Newmark displacements are estimated to be about 590 mm along the failure surface. The differences in the deformations may result from the timing of the occurrence of the initial liquefaction and degradation of the soil parameters. The coincidence of liquefaction with the onset of strong motion during the 975-year earthquake shaking is likely the reason for the good agreement in terms of displacements from the two analyses.

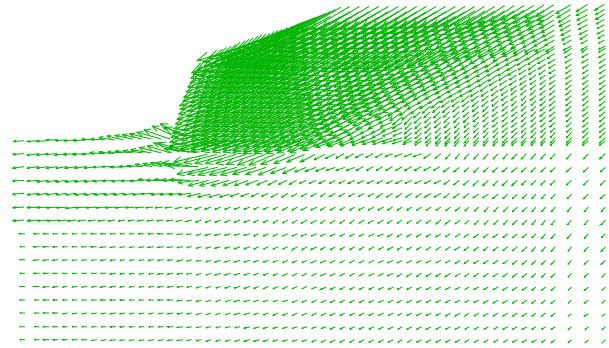

(a)

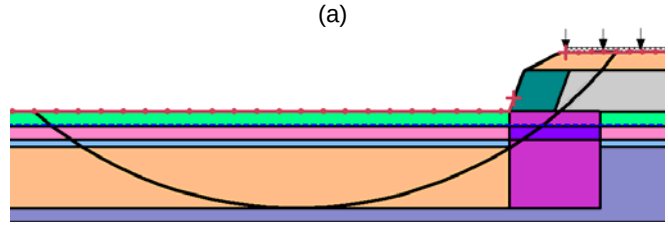

(b)

Figure 6. Critical failure surfaces from (a) displacement vectors from FLAC analyses and (b) limit equilibrium slope stability analyses.

4.3 Internal Stability

The maximum tensile forces in the geogrid elements induced by the seismic loading are summarized in Table 3. The average tensile force generated in the geogrid elements is well below the tensile yield strength. The yield strength of the geogrid is specified as being 90% of the ultimate strength with a strain limit of about 11%. The results in Table 3 indicate that the tensile forces in the geogrid elements are consistent with the level of deformation exhibited by the reinforced slope.

4.4 Design Considerations

The reinforced slope was designed in accordance with the AASHTO standard guidelines which are based on the Mononobe-Okabe (M-O) method (Appendix A). According to the AASHTO recommendations, it is acceptable to select a horizontal seismic coefficient (k_h) equal to one-half of the peak horizontal ground acceleration (PGA). The results of the FLAC analyses indicate that the maximum horizontal acceleration at a point equivalent to the centroid of the Rankine active wedge behind the slope is in the range from 0.42*PGA to 0.56*PGA, which is consistent with the AASHTO guidelines. The Rankine active wedge and the corresponding PGA results from the FLAC analyses are presented in Figure 7 and are summarized in Table 4.

Table 3. Summary of maximum tensile forces in geogrid

Geogrid number	Geogrid type	Maximum Tensile Forces (kN/m)	Average (kN/m)	Tensile yield strength (kN/m)
1	UX1600MSE	22.2 - 41.1	30.7	129.6
2	UX1600MSE	27.2 - 36.9	30.9	
3	UX1600MSE	22.5 - 33.8	28.3	
4	UX1600MSE	22.5 - 30.7	25.4	
5	UX1600MSE	20.5 - 29.1	23.9	
6	UX1600MSE	19.5 - 27.4	22.8	
7	UX1600MSE	18.5 - 25.7	21.0	
8	UX1500MSE	14.5 - 19.3	15.9	102.6
9	UX1500MSE	14.7 - 18.3	15.6	
10	UX1500MSE	14.2 - 19.0	16.1	
11	UX1500MSE	13.5 - 17.2	15.5	
12	UX1500MSE	11.9 - 16.2	13.6	
13	UX1500MSE	11.2 - 23.2	14.1	
14	UX1500MSE	10.3 - 22.3	14.1	
15	BX1120	3.8 - 6.3	4.4	17.1
16	BX1120	2.4 - 5.8	3.2	
17	BX1120	1.5 - 6.1	2.4	
18	BX1120	0.6- 7.0	1.9	
19	BX1120	0.1 - 16.5	2.9	

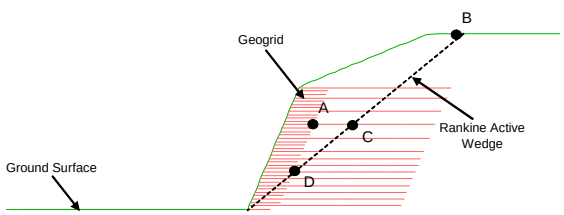

Figure 7. Rankine Active Wedge

Table 4. Summary of PGA from the FLAC analyses.

Location	Input PGA k_h* (g)	PGA from FLAC, k_h (g)	k_h / k_h* (Average)
Point A	0.355	0.148 - 0.198	0.42 - 0.56 (0.48)
Point B		0.169 - 0.229	0.48 - 0.65 (0.55)
Point C		0.139 - 0.197	0.39 - 0.55 (0.47)
Point D		0.132 - 0.171	0.37 - 0.48 (0.43)

This may be because the deformations of the geogrid reinforced slope are such that the Mononobe-Okabe assumption of the development of the active pressure holds and this allows a reduction of the seismic pressure on the back of the wall. This may not be the case for stiffer wall systems where sufficient levels of deformation do not occur and the active wedge cannot be developed.

5 CONCLUSIONS

The non-linear displacement-based FLAC modeling provides an additional understanding of the seismic performance of the reinforced slope wall and design procedures. Based on a comparison of the results from FLAC analyses performed for several Sierra Slope geometries, it would appear that the proprietary design approach provides a design that is conservative with respect to the results from detailed soil-structure interaction analyses, at least for the specific ground conditions, slope geometry and input motions analyzed herein. For the analyses performed, this is considered to be the case since the geogrid reinforced slope provides a flexible response under earthquake loading that is consistent with the assumptions employed in the code-based design approaches.

The FLAC analyses provide an indication of the time-history variations of pore pressure development and liquefaction triggering during seismic events. Forces in the geogrid can also be tracked in the analysis. The estimated forces in the geogrid did not exceed the yield strength of the reinforcement for any of the 975-year earthquake records. In addition, the results for the slope in question have shown that the global and internal stability of the reinforced slope using the standard code-based design approaches are considered to be appropriately conservative relative to the numerical modeling, at least for the conditions analyzed.

6 ACKNOWLEDGEMENTS

The analyses presented form part of a study performed for Kiewit Flatiron Partnership to provide criteria for input to the design basis for walls under seismic loading. The analyses, however, do not refer to any specific structure. The authors are grateful to Don Bose, Keith Threadkell and Nannan Yu of H5M (Hatch Mott MacDonald and MMM Group design team) for their input to the wall analyses and general contribution to the content of the paper. The assistance of Mr. German Cajigas of Nilex is also acknowledged.

7 REFERENCES

AASHTO 2002. Standard Specifications for Highway Bridges, 17th Edition, American Association of State Highway and Transportation Officials.

ATC/MCEER 2006. Liquefaction Study Report and Design Examples, Companion Documents to the Recommended LRFD Guidelines for the Seismic Design of Highway Bridges, Applied Technology Council and the Multidisciplinary Center of Earthquake Engineering Research, State University of New York.

Byrne, P.M. 2007. Dynamic analysis for modeling soil and soil-structure systems subjected to earthquake shaking. Short Course Note, June 4 to 5, University of British Columbia.

EPRI 1993. Guidelines for determining design basis ground motions. Palo Alto, Calif: Electric Power Research Institute, Vol. 1 to 5, EPRI TR-102293.

Itasca Consulting Group 2008. FLAC – Fast Lagrangian Analysis of Continua. Users Guide, Version 6.0, Minneapolis, USA.

Newmark, N.M. 1965. Effects of earthquakes on dams and embankments. Geotechnique, Vol. 15, No. 2, pp. 139-160.

Vucetic, M. and Dobry, R. 1991. Effect of soil plasticity on cyclic response. ASCE Journal of Geotechnical Engineering, Vol. 117, No. 1, pp. 89-107.

Youd, T.L., Idriss, I.M., Andrus, D.R., Arango, I., Castro, G., Christian, T.J., Dobry, R., Finn, W.D.L., Harder, L.F. Jr., Hynes, E.M., Ishihara, K., Koester, J.P., Liao, S.S.C., Marcuson, W.F.III, Martin, G.R., Mitchell, J.K., Moriwaki, Y., Power, M.S., Robertson, P.K., Seed, R.B., and Stokoe, K.H.II. (2001). "Liquefaction Resistance of Soils: Summary Report from the 1996 NCEER and 1998 NCEER/NSF Workshops on Evaluation of Liquefaction Resistance of Soils." ASCE, *Journal of Geotechnical and Geo-Environmental Engineering*, October, pp. 817-832.

APPENDIX A

A.1 REINFORCED SLOPE DESIGN METHODOLOGY

The design of the Sierra Slope structures generally follows the methods and guidelines stated in FHWA-NHI-00-043 "Mechanically Stabilized Earth Walls and Reinforced Soil Slopes Design and Construction Guide", Bishop's Modified Method of limit equilibrium slope stability analysis (Bishop, 1955), and the specific project specifications. In B.C., the design is also required to comply with the AASHTO Standard Specifications for Highway Bridges.

The FHWA-NHI-00-043 document defines a reinforced soil slope as having a face inclination less than 70 degrees. The AASHTO Standard Specifications for Highway Bridges, 17th Edition, 2002 (AASHTO 2002) generally adopt into the specifications the guidance in FHWA-NHI-00-043 for walls, but do not provide specifications for slopes. Moreover, AASHTO 2002 defers to FHWA-SA-96-071 for items not specified in detail (e.g., Section 5.8, p.138 for the discussion of complex geometries). FHWA-NHI-00-043 is the successor document to FHWA-SA-96-071; the title remained the same.

Computational programs developed to carry out limit equilibrium slope stability analysis are used to evaluate internal and external circular failure surfaces for MSE slopes. Global stability can also be analyzed using the same software.

The minimum factors of safety with respect to failure modes used in the Tensar design are listed in Table A1; the factors are higher than the minimum values recommended by the FHWA to comply with the project specifications.

A.2 STRUCTURAL GEOGRID

Uniaxial (UX) geogrids are manufactured using select grades of high-density polyethylene (HDPE) resins that resist elongation (creep) when subjected to high loads for long periods of time. These geogrids carry large tensile loads applied in one direction (along the roll), and their open aperture structure interlocks with natural fill materials.

Biaxial (BX) Geogrids are manufactured using select grades of polypropylene or copolymers that resist moderate loads over long periods of time. These products carry loads applied in any direction in the plane of the geogrid. BX geogrids are used as intermediate reinforcement between layers of stronger UX geogrids or as a wrap material for stability at the face of the structure. When used as a wrap, the polymers used to manufacture the BX geogrids include a UV-stabilization additive package.

Table A2 reports the types of geogrids used along with their tensile properties for a 75-year design life.

Table A1. Minimum Factors of Safety

Internal Stability	Static	Rapid Drawdown	Seismic (975-yr)
Geogrid Tensile Strength, Minimum	1.5	1.1	1.2
Geogrid Pullout Capacity, Minimum	1.5	1.1	1.2
Surficial Stability, Minimum	1.5	N/A	1.2

Table A2. Geogrid Properties

Geogrid Type	T_{ult} kN/m	RF_{cr}	RF_{id}	RF_d	T_{al} kN/m	C_i
UX1500MSE	114.0	2.6	1.10	1.10	36.2	0.8
UX1600MSE	144.0	2.6	1.10	1.10	52.7	0.8
BX1120	19.0	3.60	1.10	1.10	4.4	1.0

T_{ult} = Ultimate tensile strength

RF_{cr} = Reduction factor for creep for 120-year design life

RF_{id} = Minimum reduction factor for installation damage

RF_d = Minimum reduction factor for durability

T_{al} = Allowable tensile strength

C_i = Interaction Coefficient